INSTITUT DE FRANCE
Académie des sciences

Comptes Rendus
Mécanique

Thaer Syam, Yousif Badri, Omran Abdallah, Sadok Sassi, Jamil Renno and Omar D. Mohammed

Towards a simplified technique for crack recognition in gearing systems

Volume 350 (2022), p. 477-494

Published online: 28 September 2022

https://doi.org/10.5802/crmeca.128

Les Comptes Rendus. Mécanique *sont membres du Centre Mersenne pour l'édition scientifique ouverte*
www.centre-mersenne.org
e-ISSN : 1873-7234

Comptes Rendus
Mécanique
2022, Vol. 350, p. 477-494
https://doi.org/10.5802/crmeca.128

Synthesis / *Synthèse*

Towards a simplified technique for crack recognition in gearing systems

Thaer Syam [a], Yousif Badri [b], Omran Abdallah [b], Sadok Sassi [*, b], Jamil Renno [b] and Omar D. Mohammed [c]

[a] Department of Mechanical Engineering, Texas A&M University, 3123 TAMU, College Station, TX 77843, USA

[b] Department of Mechanical Engineering, Qatar University, Qatar

[c] Mechanical Engineering Department, College of Engineering, Prince Mohammad Bin Fahd University PMU, Saudi Arabia

E-mails: ts1405457@student.qu.edu.qa (T. Syam), yb1903174@student.qu.edu.qa (Y. Badri), oa1515810@student.qu.edu.qa (O. Abdallah), sadok.sassi@qu.edu.qa (S. Sassi), jamil.renno@qu.edu.qa (J. Renno), osily@pmu.edu.sa (O. D. Mohammed)

Abstract. This paper presents a simple and effective method to identify and quantify the existence of cracks in the teeth roots of spur gears. The problem was numerically analyzed through finite element-based simulation with SolidWorks in the first part of this work. The computed tooth in-plane bending stiffness and natural frequency decreased considerably with an increase in the crack length, while the deformation followed an opposite trend. The numerical results were experimentally validated through a convenient and straightforward test rig developed for this purpose. The experimental results obtained from the modal analysis tests confirmed the previously obtained numerical results. A graphical representation of these parameters on a polar plot shows concentric circles with no particular sign from one tooth to another. However, in the presence of cracks in the vicinity of teeth roots, these circular patterns became deformed in the neighborhood of the teeth with defect, which provides a quick and easy visual check to detect a crack and quantify its extent.

Keywords. Gears, Crack detection, Mapping, Modal analysis, Finite element analysis.

Manuscript received 31 May 2022, revised 13 August 2022, accepted 6 September 2022.

1. Introduction

Gears have been used in machines to transmit power and motion for many years and are now among the most common components in mechanical engineering systems. They constitute a significant part of any rotating system because of their ability to transmit motion and high torque between shafts in different configurations (parallel, intersecting, and non-intersecting) with high efficiency and low energy loss. However, various faults may occur within the gear transmission system because of severe operating conditions. In the literature, it has been reported that defects

* Corresponding author.

in the gears represent 80% of issues in transmission systems and 10% of the problems in rotary machines [1]. These defects may result from several factors ranging from inadequate lubrication, inaccurate manufacturing, friction, fluctuating loads, misalignment, poor cooling, or poor installation procedures, among others [2]. In harsh conditions, gears are designed to be efficient without adding extra weight [3]. Therefore, gear teeth must be adequately strong and resistant to wear but have a thin rim. However, narrow rims are prone to gear tooth fatigue as a result of bending. In gear systems, bending fatigue is the most common cause of fatigue failure [4]. Indeed, fractures in gear teeth often begin in the root fillet because a cantilever beam's weakest point is at its base [5]. Frequently, cracks on gears occur through fatigue caused by cyclic loading. Fatigue stress is mainly concentrated at the root of the teeth because of the small tooth fillet radius. Besides, it progressively damages the gear teeth, resulting in tooth failure. If any tooth fails, the whole gearbox is in danger of failure in a short time, resulting in costly losses.

Once a crack has initiated, it expands either towards the foot of the tooth or inside the rim. In some systems, such as in aircraft, cracking inside the rim can be disastrous, as this would cause a propeller or rotor to disengage [6]. Approximately 60% of gear damage results from local fatigue in the teeth [7, 8]. However, according to Allianz Versicherungs-Aktiengesellschaft [9], the fatigue damage in the teeth could be more severe and may even reach 90% of the deterioration in gears. It is possible to determine the severity of damage by knowing the crack width relative to the tooth width, how many cracks are present in each gear, and other parameters. Therefore, within the field of gear design, crack propagation has attracted widespread interest in enhancing safety and preventing casualties.

In industry, monitoring the condition of gears is essential. Defects in the gear mesh may produce unacceptable loud noise and vibration levels, disturb workers on the worksite and affect their hearing, and cause failures in the machinery, which cause severe losses. In addition, failures in the gear mesh reduce the efficiency, thus, decreasing industrial operation productivity. Generally, faults in a gearbox change the normal operating conditions and strongly affect a system's production rate [10]. Therefore, monitoring the health of the gear mesh is vital [11, 12], and early detection of gear cracks is needed to avoid all these issues and predict the time of failure, which presents the need for a method or a technique to detect and precisely determine the severity of tooth cracks. Moreover, several techniques are suggested for minor damage and/or high frequency both from the experiment and post-processing point of view [13, 14].

Recent research has attempted to predict the paths of gear cracks. Several techniques based on Linear Elastic Fracture Mechanics (LEFM) have been proposed [15]. Shuting [16] investigated the propagation path of a crack in a spur gear by developing a FORTRAN code for use with a finite element (FE) program and a LEFM method. This code spontaneously reproduced a gear section with three teeth in a row that had fine meshing and a crack at the foot of one tooth. However, extensive computation was needed to evaluate the essential stress intensity factor to predict the growth of the crack. The same author [17] also analyzed the effects of gear rim thickness and gear torque on the crack's propagation angle and direction and used an experimental gear test rig to support the proposed method. The combination of LEFM and FE techniques, based on fracture analysis code (FRANC), assuming an initial crack on the foot of the gear, was able to calculate the first mode (I) of the stress intensity factor and made it possible to simulate the direction of the crack propagation.

Moreover, Hui *et al.* [18] used the FE technique to analyze crack extension within a gearbox and confirmed the results through experiments. Numerically, cracking could be predicted by applying fracture mechanics and estimating the stress intensity factors, which could be determined by the virtual crack extension method. Furthermore, the simulation and the experiment agreed well regarding crack growth direction. Finally, Zhiguo *et al.* [19] and Xihui *et al.* [20] developed new analytical models for calculating the mesh stiffness that simulated crack propagation and

depth as well as the tooth width. This study extended the analytical calculation models for mesh stiffness in cracked gears from 2D to 3D.

Chaari *et al.* [21] also produced crack propagation in multi-dimensional structures. Their models first approximated a cracked geometry, and then the boundary element method was used to determine the stress intensity factors. The precision of the stress intensity factors determined how accurately crack growth was predicted. Chaari *et al.* [22] also developed FE and weight function techniques to evaluate stress intensity factors. Yang and Lin [23] developed a 2D FE method that applied the principle of linear elastic fracture mechanics and used this to investigate the path of crack propagation in pairs of gears with different contact ratios. Wu *et al.* [24] used a 2D fracture analysis code for FE software and LEFM to simulate crack propagation in a spur gear tooth. These models included 2D, and 3D FE cracked gear tooth specimens. Both methods agreed well with the experimental results.

Different scenarios of gear crack propagation were described and explored in [24–26]. In order to study the dynamic response of a cracked gear, the mesh stiffness of a time-varying gear was calculated and explained in [27, 28].

The use of natural frequencies for gear tooth crack detection was studied in [29, 30]. In these research works, the frequency response functions (FRFs) and time-frequency analysis were applied to investigate the shift in natural frequencies with crack propagation. The authors concluded that FRFs could be used for gear tooth crack detection. In simulations of different cracking cases, the FRF changed in the mesh segments as the mesh stiffness varied. The results were obtained by dynamic modeling and were not proved experimentally.

In the current work, a combination of numerical and experimental investigations was considered to assess how tooth cracks affected the dynamic response of a spur gear. A test rig was built to examine the use of natural frequencies for gear crack detection. Nine cases involving different numbers of cracks and different crack types, lengths, and locations were considered.

2. Gear cracks and crack detection method

2.1. *Crack detection method*

The crack detection method used in the current work aims to detect crack initiation in gear teeth by examining the vibration response's amplitude and frequency. These cracks differ in their depth, location, and number. The fault detection analysis is based on a comparative approach between FE simulation and experimental modal analysis.

Figure 1 shows the specifications of the set of gears, along with the dimensions used in the analysis. Besides the healthy gear, eight defective gears are considered in the present investigation, which differ in the number of cracks, locations, and crack length percentages (CLP%). The material of the gear is cast carbon steel.

2.2. *Crack propagation scenarios*

Two different propagation paths are generally considered as a crack grows and propagates deep inside the tooth width (Figure 2). The first scenario, marked in red, is a straightforward path where the crack propagates through the tooth itself, from one face to the other, between the opposite root locations. In the second scenario, marked in blue, the crack propagates through the rim at an angle of 35°. In all cases, the crack thickness is 0.2 mm. Therefore, if CL indicates the actual crack length and PL is the total crack length path, we can use (1) to calculate the CLP%:

$$\mathrm{CLP} = \frac{\mathrm{CL}}{\mathrm{PL}} \times 100. \tag{1}$$

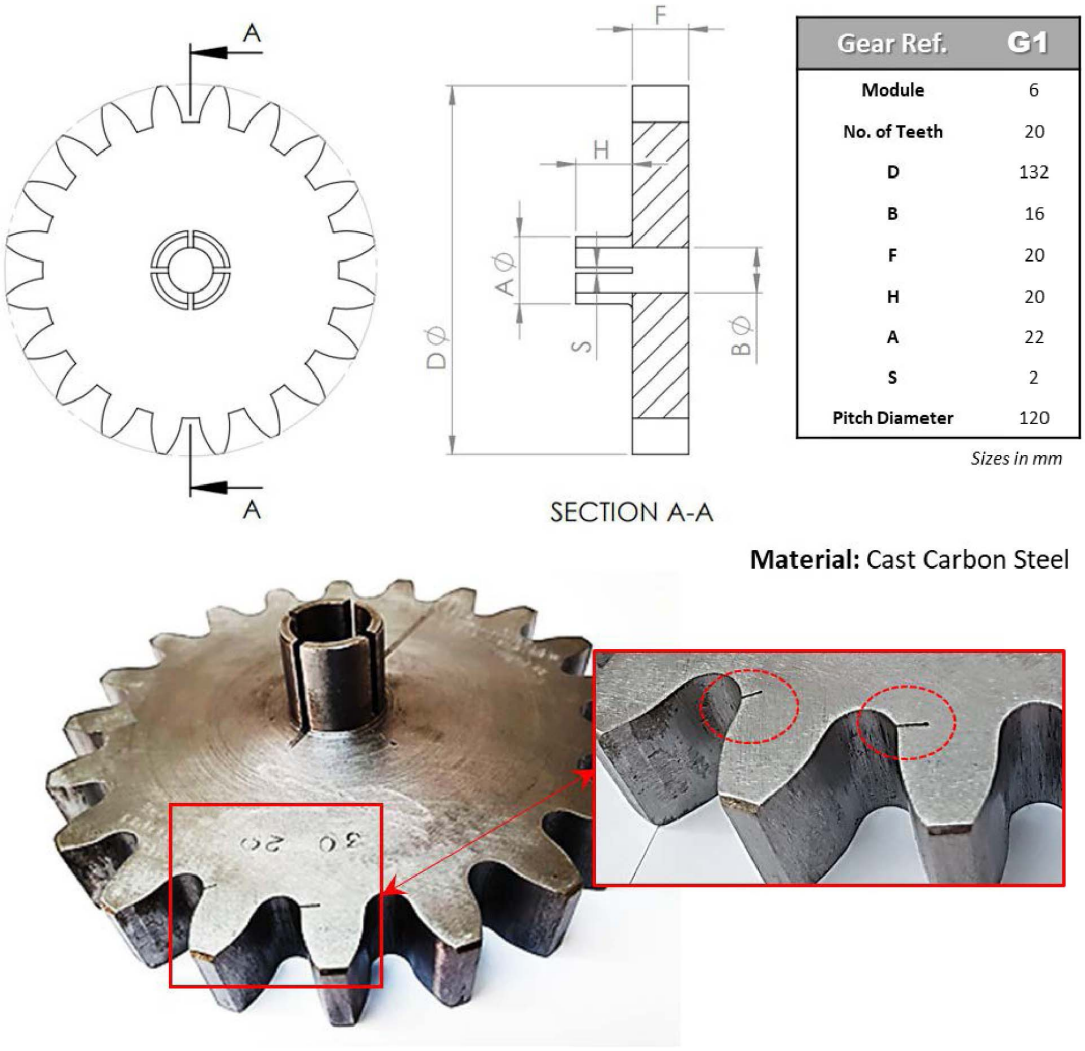

Gear Ref.	G1
Module	6
No. of Teeth	20
D	132
B	16
F	20
H	20
A	22
S	2
Pitch Diameter	120

Sizes in mm

Figure 1. Gear specifications.

In this study, nine cases were considered, where the technique of Electric Discharge Machining (EDM) was used to intentionally seed artificial cracks with CLP% varying from 0% to 50%. Table 1 summarizes all the cases considered in the present investigation.

3. Numerical modeling of gear tooth cracks

During experimental analysis of a gear's dynamics, prior knowledge of the frequency range of interest is always beneficial for reducing the amount of time required and enhancing the accuracy of the results. Therefore, a numerical pre-study based on FE analysis (FEA) is required to obtain the frequency zone of interest where the natural frequency of tooth in-plane bending lies.

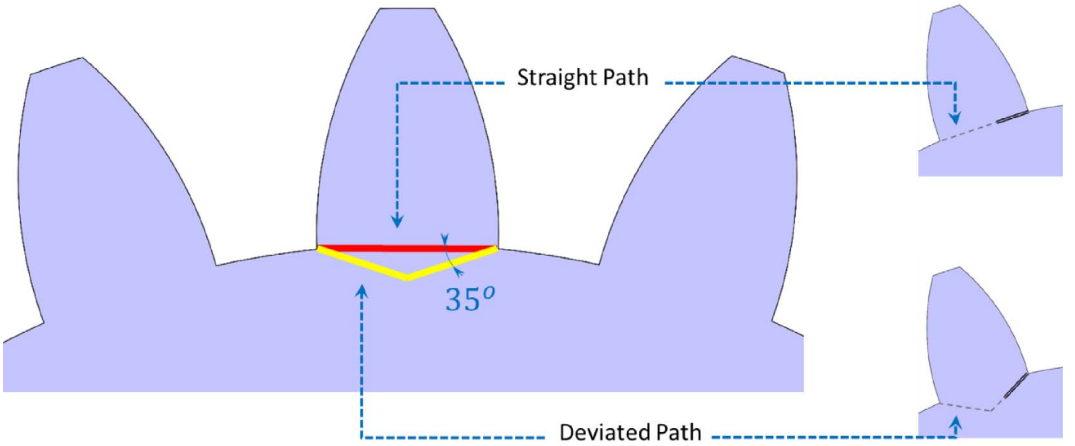

Figure 2. Crack propagation details: straight and deviated paths.

Table 1. Details of gear cracking cases

Gear ref.	Case	Number of cracks	CLP (%)	Crack propagation angle (°)	Crack location
1	Healthy	0	0	0	–
2	Cracked (single)	1	10	0	On one tooth
3	Cracked (single)	1	20	0	On one tooth
4	Cracked (single)	1	30	0	On one tooth
5	Cracked (single)	1	40	0	On one tooth
6	Cracked (single)	1	50	0	On one tooth
7	Cracked (multiple)	2	20 and 30	0 and 0	On two teeth separated by 180°
8	Cracked (multiple)	2	20 and 30	0 and 35	On two teeth separated by 90°
9	Cracked (multiple)	2	20 and 30	35 and 0	On two consecutive teeth

3.1. *Gear modeling*

All gears were designed with SolidWorks® software. Figure 3 shows the initial 3D CAD drawing of the healthy gear (with no cracks). For each of the defective cases, the crack was initiated on the right-hand face of the tooth.

3.2. *Boundary conditions*

The boundary conditions of this study are straightforward. The main aim was to capture the natural frequency of the deformed tooth while keeping the remainder of the gear's body fixed. Therefore, the gear was fully fixed on the inner diameter (in contact with the supporting shaft). In addition, one of the lateral surfaces was prevented from moving in the perpendicular direction. Such supporting conditions intend to exclusively highlight the vibration modes for the teeth in-plane bending deformation.

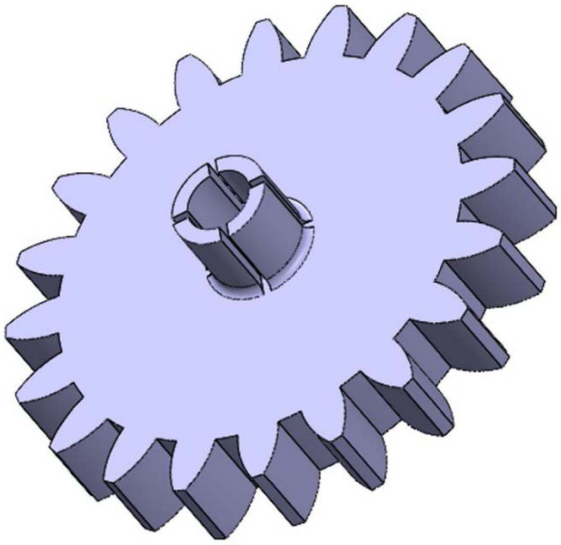

Figure 3. The 3D-CAD model of a healthy spur gear.

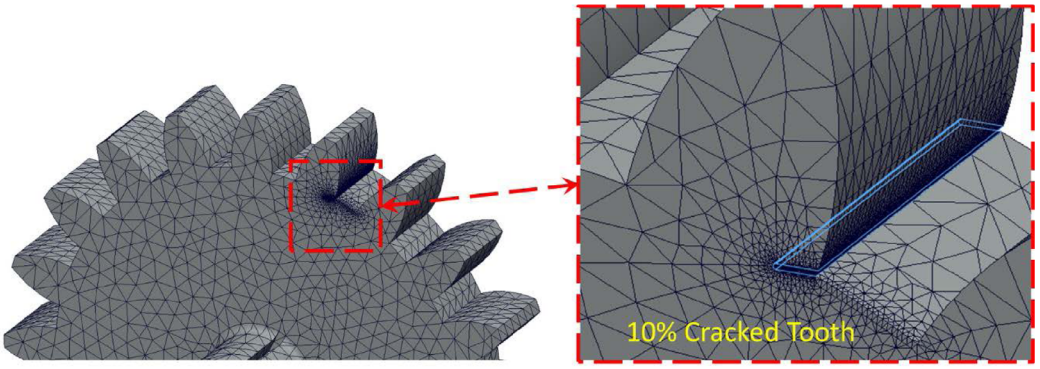

Figure 4. Meshing for the cracked tooth using Mesh Control.

3.3. *Meshing*

Meshing is vital to processes of computer-aided engineering simulation. The accuracy, convergence, and speed of reaching a solution are all directly influenced by the mesh. Unfortunately, creating and meshing a model usually take up a large amount of the time to obtain results through computer-aided engineering design. Better solutions can be obtained with improved and more automated meshing tools. However, in a cracked gear, the crack area and the place where the force is applied are tiny. Therefore, the mesh density in these places was increased by applying the "Mesh Control" feature of SolidWorks. This feature is used to increase the number of elements locally in the vicinity of the tiny cracked area. Figure 4 shows an example of a cracked gear (G2) in which the number of elements was locally increased to better approximate the results. Table 2 shows the meshing properties for all of the nine cases in SolidWorks.

Table 2. Meshing properties and statistics in SolidWorks for all gears

Case	Element type	Integ. points	Max. element size (mm)	Min. element size (mm)	No. of nodes	No. of elements	Elements with an aspect ratio < 3 (%)
1	Parabolic tetrahedral	4	0.25	0.005	2,089,674	1,484,625	99.9
2					2,087,781	1,482,673	99.7
3					2,085,888	1,480,721	99.7
4					2,083,995	1,478,769	99.7
5					2,082,102	1,476,817	99.7
6					2,080,209	1,474,865	99.6
7					2,073,316	1,471,913	99.5
8					2,071,423	1,464,961	99.8
9					2,068,530	1,413,019	99.4

Table 3. The natural frequency of tooth bending for all gears

Gear	Gear number	CLP%	Natural frequency of tooth bending (Hz)
1	Healthy	0	24,272
2	Cracked (single)	10	24,139
3		20	23,853
4		30	23,312
5		40	21,753
6		50	18,164
7	Cracked (multiple)	20	23,862
		30	23,302
8		20	23,851
		30	23,402
9		20	23,923
		30	23,322

3.4. *FEA results and discussion*

For the sake of reference, the case of a healthy gear (with no cracks) was initially considered. Among all the modes of vibrations, only the ones showing the in-plane deformations were considered because of the boundary conditions. The particular mode for which the rim is stationary and the teeth are bending is the one to be focused on in the simulations since it is related to teeth in-plane bending. As shown in Figure 5, such mode was found to be excited at a frequency of 24,268 Hz.

Similar simulations were subsequently performed for damaged gears with single and multiple cracks. All cracks were considered to progress through the gear tooth with no propagation angle. Table 3 shows the simulation results of all cases. Overall, one can see that there was good consistency in the accuracy of the results. For example, the natural frequency of a cracked tooth with 20% CLP was 23,853 Hz for G3 and 23,862 Hz for G7. The slight difference (around 0.4%) is simply caused by the differences in the meshing properties created by the number of cracks in gear.

To help quantify how crack depth affects the variation in the bending frequency, the frequency results were normalized to the initial value obtained from the healthy tooth and presented as a

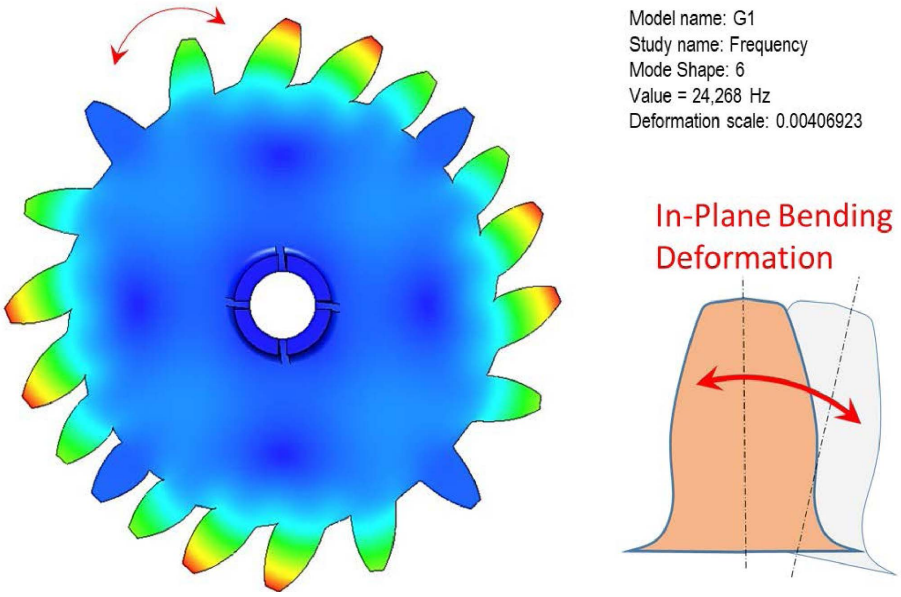

Figure 5. The first mode of tooth bending for the healthy gear (G1).

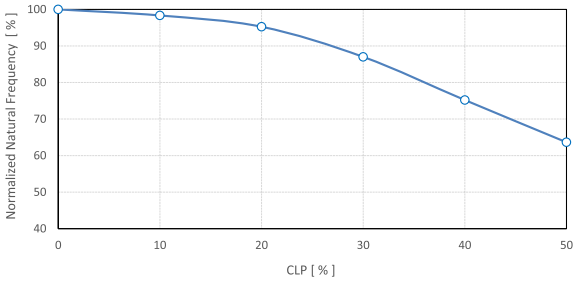

Figure 6. The natural frequency of tooth bending versus the CLP%.

percentage in Figure 6. Thus, one can see that when the crack propagates and its CLP% increases, the natural frequency of that mode decreases. For example, the natural frequency of a healthy tooth drops from 100% (24,272 Hz) to 63.64% (18,164 Hz) when the crack length increases from 0% CLP to 50% CLP. The reduction in the stiffness of the teeth can explain this frequency variation.

The natural frequency of tooth bending of the cracks for G3 (20%) and G4 (30%) were 23,853 Hz and 23,312 Hz, respectively. These cracks were propagated through the tooth itself, where no angle propagation was presented. For 20% CLP, G7 and G8 showed approximately identical results, as the crack was the same (through the tooth), with values of 23,862 Hz and 23,851 Hz, respectively. However, as displayed in Table 4, in the particular case of G9, the natural frequency increased slightly to 23,923 Hz. Such an increase, which is close to 3.3%, can be explained by the orientation of the crack. Indeed, the crack propagation through the rim makes the tooth harder to bend and slightly increases its natural frequency compared with propagation inside the tooth itself. The same applies to the case of 30% CLP% in G4 (23,312 Hz) and G8 (23,402 Hz).

Figure 7 is a graphical representation of Table 4, where the crack propagation angle effect is visible. In the case of G9, the natural frequency of the 20% cracked tooth is slightly higher than

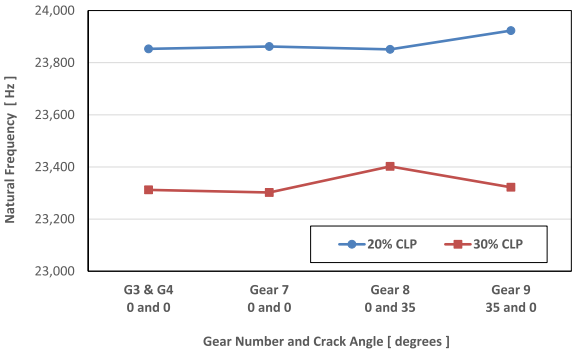

Figure 7. Influence of the angle of crack propagation on the natural frequencies of the teeth.

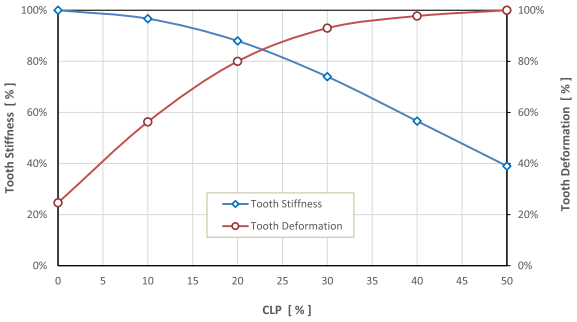

Figure 8. Stiffness and deformation vs CLP% for gears with single cracks.

Table 4. The natural frequency of tooth bending for the two cases on each gear

Gear	Case	Crack propagation angle (°)	Natural frequency of cracked teeth (Hz)	
			20% CLP	30% CLP
3, 4	Cracked (single)	0 and 0	23,853	23,312
7	Cracked (multiple)	0 and 0	23,862	23,302
8	Cracked (multiple)	0 and 35	23,851	23,402
9	Cracked (multiple)	35 and 0	23,923	23,322

the average value of the other cases where the propagation is through the tooth. Similar behavior can be noticed for the 30% CLP% crack of G8.

By applying a force in the normal direction of the tooth's surface and measuring the deformation in the same direction, one can evaluate the bending stiffness of that tooth. Figure 8 shows the stiffness and deformation percentage variation for all gears with single cracks. The stiffness decreased as the CLP% increased, whereas the deformation followed the opposite trend.

4. Experimental validation

4.1. *Experimental methodology and setup*

To validate the previous numerical developments, a test rig was designed, where an impact hammer test was used to excite and measure the tooth bending frequency. As illustrated in Figure 9,

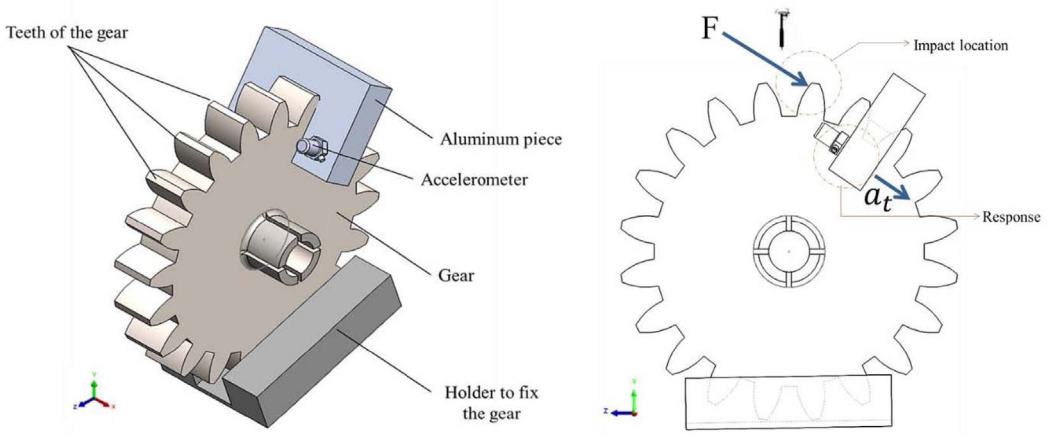

Figure 9. Methodology of the experimental work.

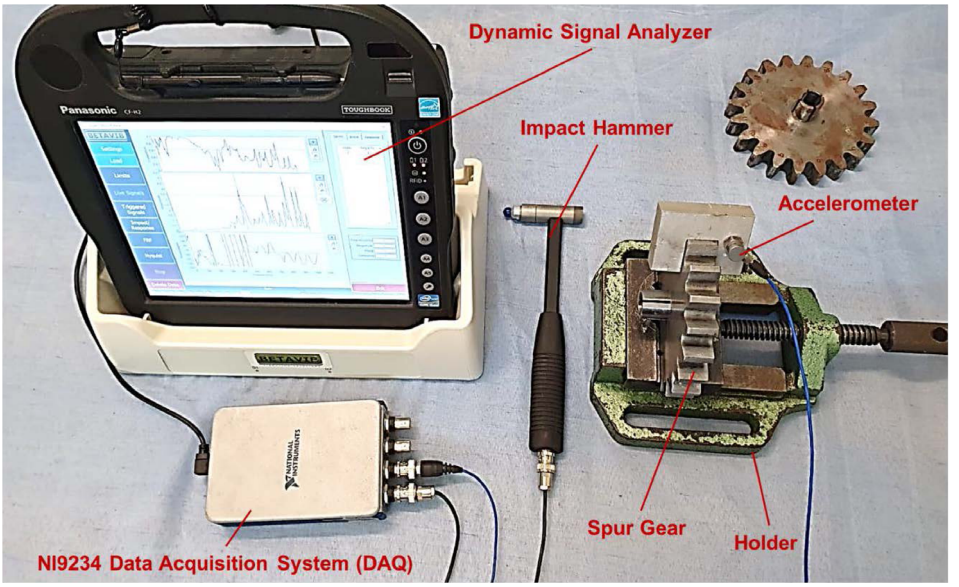

Figure 10. Experimental setup.

the gear under investigation was secured to a massive vice, with a special aluminum element attached to it in the space between two consecutive teeth. A tiny ICP-type accelerometer (Model PCB 352C33, sensitivity 101.2 mV/g) was mounted on this element to collect the vibrations in the tangential direction. The entire setup was used to measure the bending vibration of tooth i after tooth $i-2$ was excited on its tip by a Model PCB-086 impact hammer (0–500 lb; 10 mV/lb). The vibration response was collected by a data acquisition system (NI 9234) and analyzed by dedicated BetaVib software built into the tablet (CF-H2 TOUGHBOOK). Figure 10 depicts all the details of the hardware used.

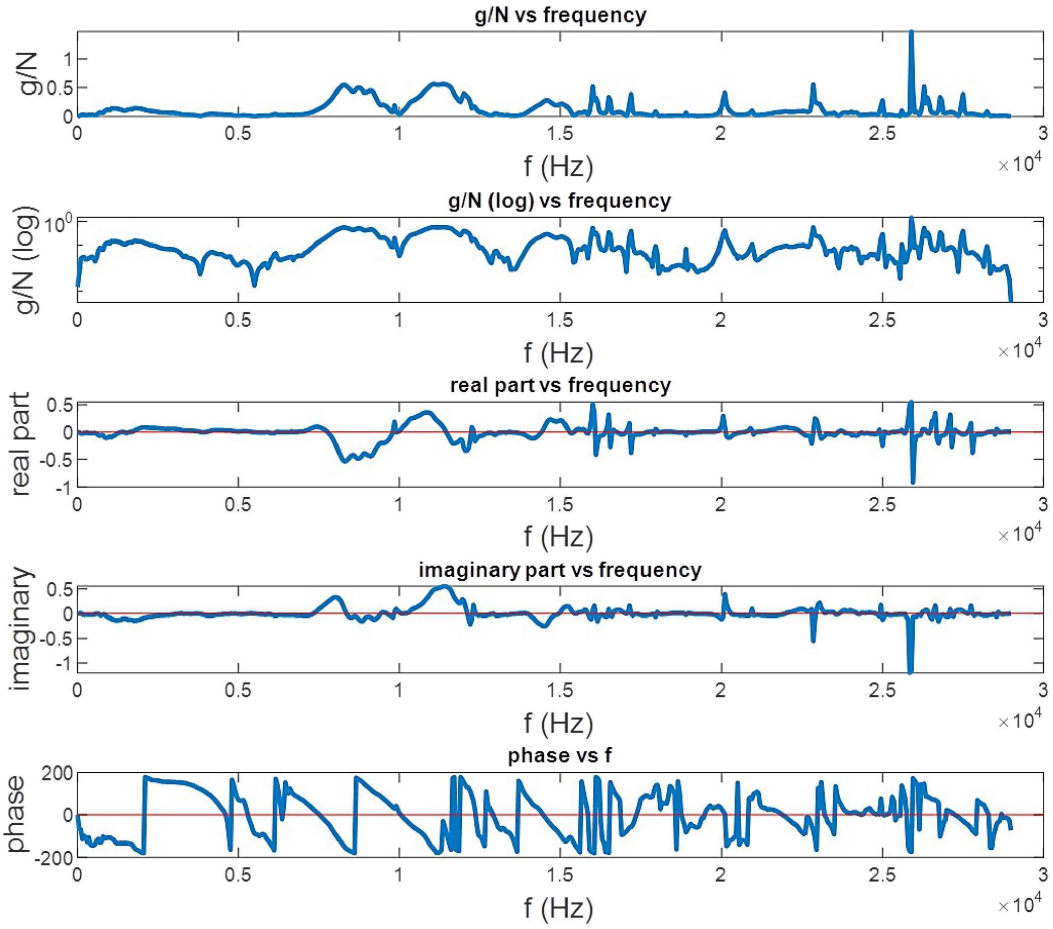

Figure 11. FRF results for G1.

4.2. *Experimental results and discussion*

Combining the input signal (hammer impact force) and the output signal (tooth in-plane bending acceleration in the tangential direction) allowed us to obtain the FRF for all the teeth of all gears and then compare them. As per the *Nyquist* theorem, the sampling frequency of reading was set to 54 kHz to allow a useful reading range of 28 kHz, higher than the limit of 24 kHz prescribed by the FE numerical simulation. To secure a high level of consistency, all FRF results were averaged three times in each case. A glance at Figure 11 portraying the FRF of the healthy gear across a broad spectrum (up to 30 kHz) shows a high density of information, as this analysis captures all modes of vibration.

Therefore, to focus exclusively on the tooth in-plane bending frequency, which is located around 24 kHz, as revealed by the FEA, a zoomed spectrum (from 20 to 29 kHz) is highly recommended. The information displayed in Figure 12 permits us to see a pronounced peak around 25.9 kHz. This experimental result is very close to the expected numerical value of 24.272 kHz. The extra pieces of information related to the real part, the imaginary part, and the phase shift indicate without ambiguity that this frequency represents the natural frequency of tooth bending.

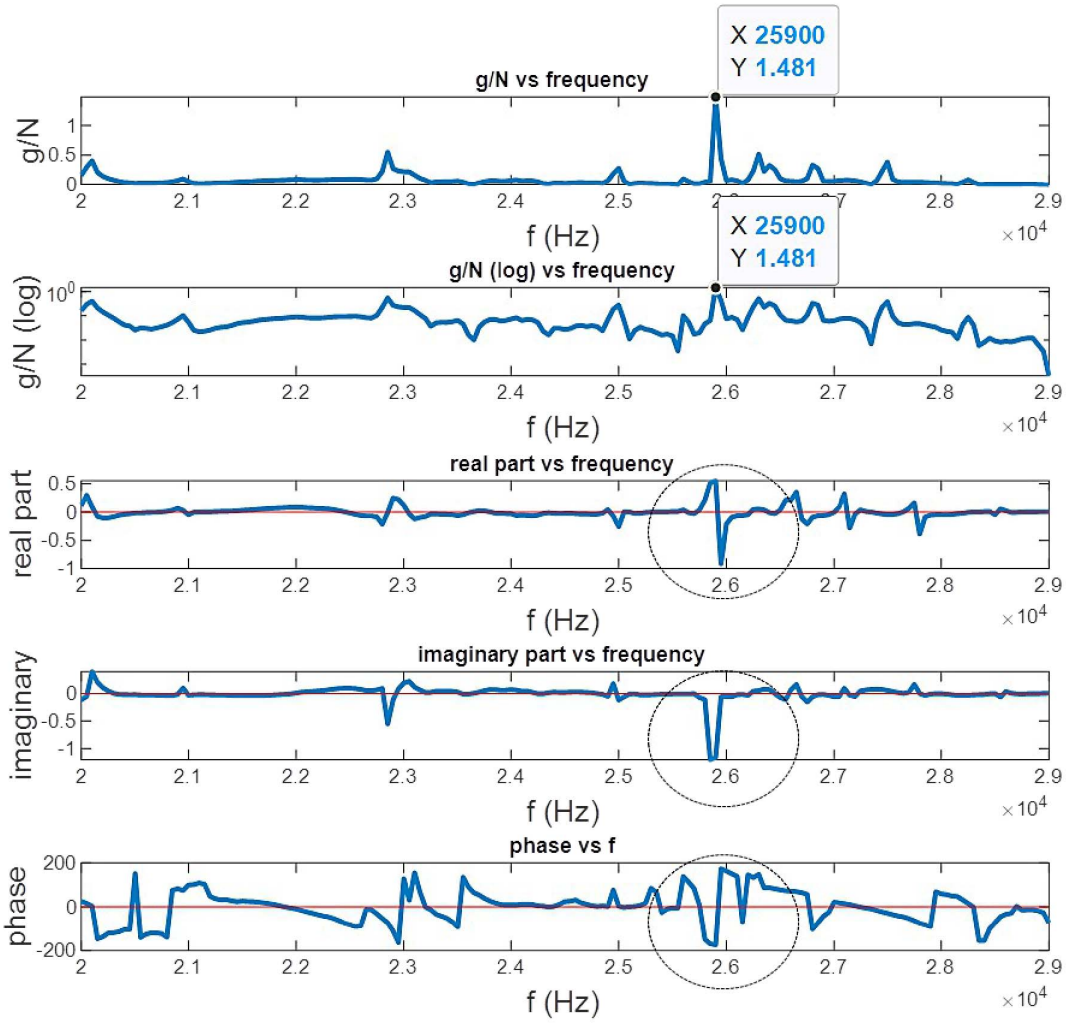

Figure 12. FRF results for G1 at a specific frequency range.

Once the natural frequency of tooth bending of the healthy gear (G1) was confirmed, the modal analysis was performed for the rest of the gears (Cases 2 to 9). A typical example of FRF curves comparing healthy (shown in blue) and damaged (shown in red) gears are displayed in Figure 13, with linear and logarithmic scales. One can see that the frequencies of cracked teeth shift to lower values, but their amplitudes are higher. Such behavior is related to the loss of stiffness created by the crack. This result agrees with the FEA results obtained earlier.

To verify both approaches, a comparison study was made. Table 5 shows the natural frequency of tooth in-plane bending obtained with FEA and experimental analysis. One can see that both sets of results have similar trends and comparable values.

5. Mapping technique for crack detection

Another interesting way of representing the previous results is using a polar plot. In such a graphical representation, the angular location of each tooth will be combined with one of its

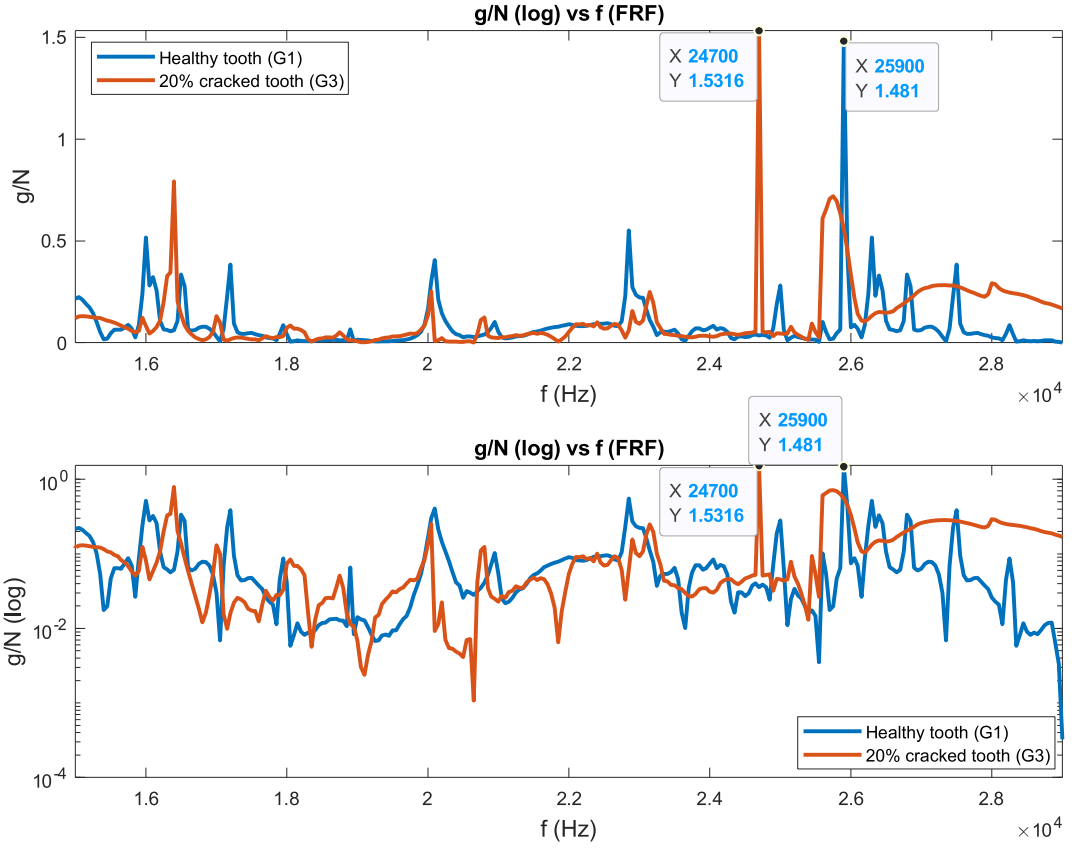

Figure 13. FRF results for the two gears, G1 (0% CLP) and G3 (20% CLP).

Table 5. Comparison between the experimental and numerical natural frequency of the in-plane teeth bending for different values of CLP%

Gear number	Case	No. of cracks	CLP (%)	Teeth natural freq. (kHz)		Relative error
				Experimental	Numerical	
1	Healthy	0	0	25.90	24.272	6.71
2			10	25.50	24.139	5.64
3			20	24.70	23.853	3.55
4	Cracked (single)	1	30	22.60	23.312	3.05
5			40	20.50	21.753	5.76
6			50	16.40	18.164	9.71

physical properties. For example, in the absence of cracks, it is assumed that all healthy teeth (19 teeth) will have the same behavior, and the plot contour will look like a perfect circle. Figure 14 shows the the polar plot strategy in identifying the cracked tooth of the gears. Since the number of teeth for all gears is 20 teeth, the polar plot was divided into 20 points which represent the teeth location of the gear. However, any deviation from the healthy condition will result in variation of the measured parameter and, consequently, a noticeable distortion in the polar plot. For example, Figure 15 shows the polar plot of deformation amplitude and natural frequency for all gears with single crack (G1 to G6) cases.

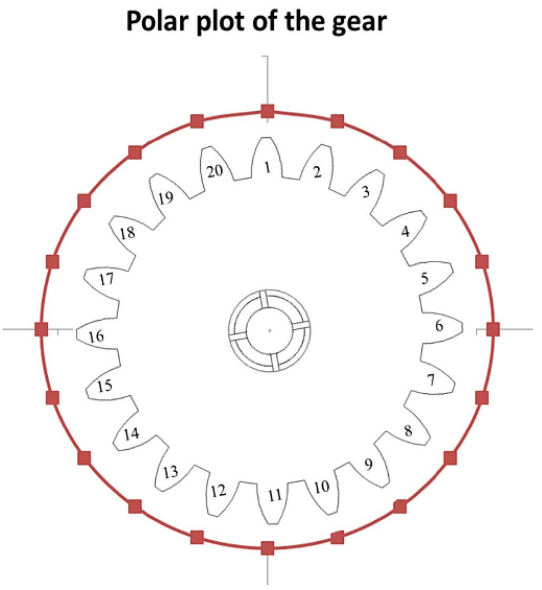

Figure 14. Polar plot explanation along with teeth numbering.

As can be seen, each plot consists of two circles: the blue one represents the deformation amplitude of each tooth, and the red one represents the natural frequency of tooth bending. The representation of both parameters in one common plot is achieved by scaling both values. For better visualization, the deformation amplitude values are presented as polar coordinates with a radius of two units, whereas the frequency values are with a radius of one unit.

In Figure 15a, both circles look perfect, as the set of teeth is not suffering from any imperfection, and the readings are the same from one tooth to another. However, when a single crack is noticed on one tooth (Figure 15b–f), a distortion in both circles can be observed in the immediate vicinity of that tooth's angular position. The more considerable the crack, the more the distortion noticed in the polar representation.

In the presence of multiple cracks, polar graphical representations can also be used to monitor the existence of numerous cracks. Indeed, as shown in Figure 16, the distortion of the concentric circles suggests the coexistence of several cracks simultaneously. For example, a glance at Figure 16a shows the polar plot of G7, where an angle of 180° separates two cracks. Although this representation method is not quantitative, the difference in the peak amplitude variations of both circles indicates that the lower crack is more pronounced. In this case, a 20% CLP is present in the upper tooth and a 30% CLP in the lower one. The use of any artificial intelligence technology could solve this issue. For G8, represented in Figure 15b, the two cracks are clearly separated by an angle of 90°. When the two cracks are consecutive, such as in the case of G9, the polar plot of Figure 16c is not as sharp as in the previous cases. The variation in the curvature of the circles suggests that the tooth on the left (30% CLP) is more damaged than the one to the right (20% CLP).

6. Conclusion

The primary aim of this study was to develop a quick and efficient means of analyzing the dynamic behavior of spur gears to recognize the existence of cracks that corrupt the damaged teeth.

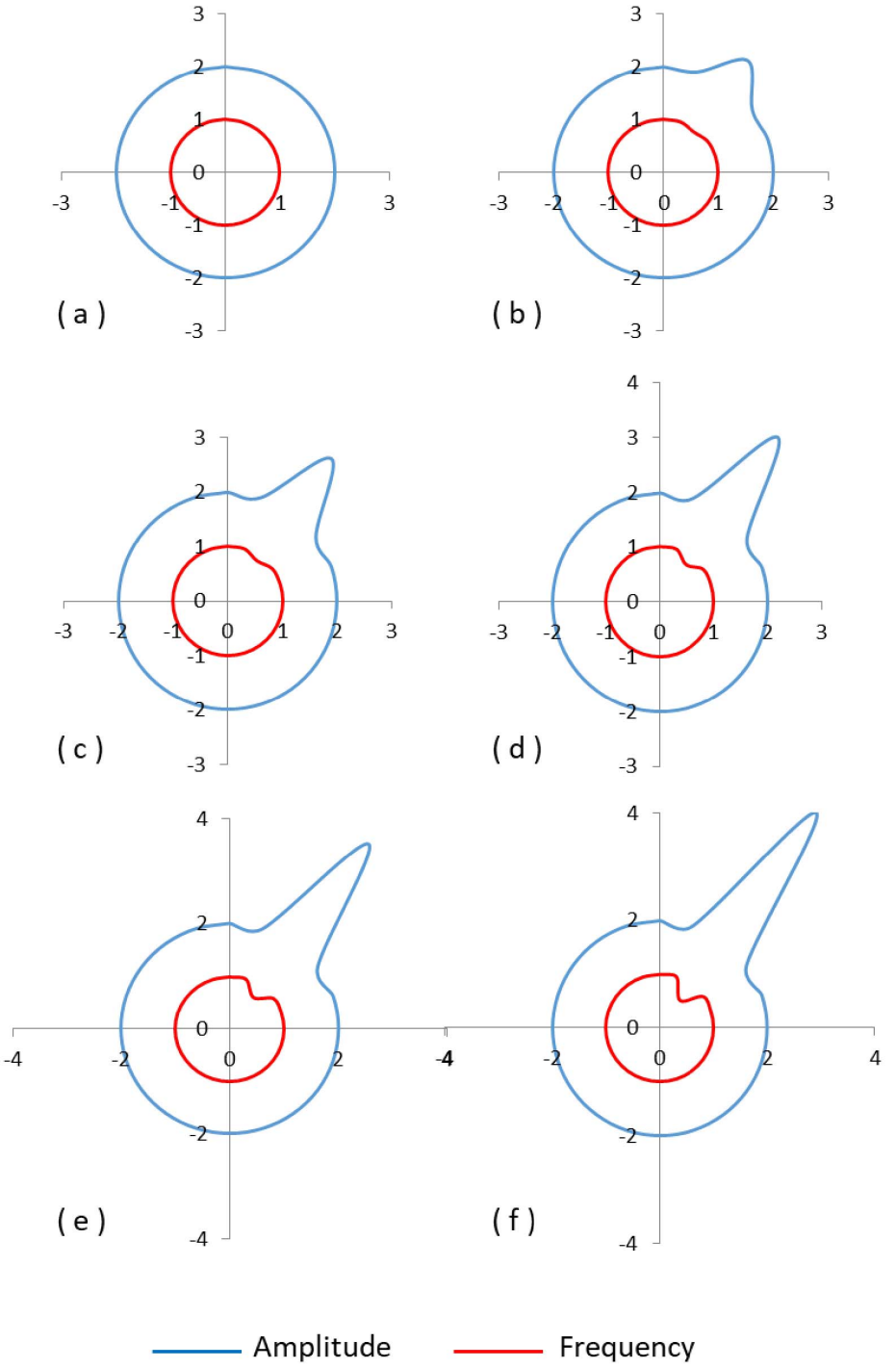

Figure 15. Polar plots from SW simulations for the amplitude and frequency of each gear. (a) G1 (0% CLP%); (b) G2 (10% CLP); (c) G3 (20% CLP); (d) G4 (30% CLP); (e) G5 (40% CLP); and (f) G6 (50% CLP).

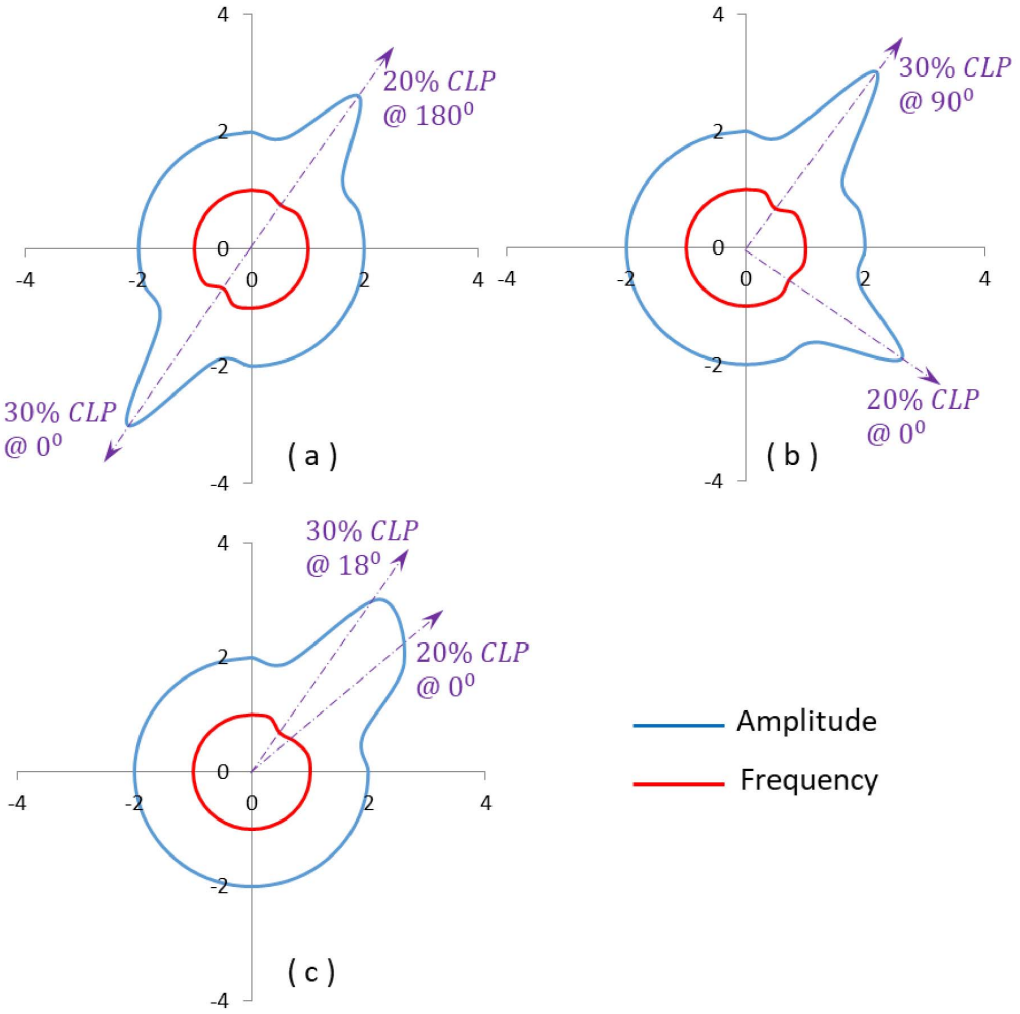

Figure 16. Polar plots from SW simulations for the amplitude and frequency of each gear. (a) G7 (20% CLP @ 0° and 30% CLP @ 180°); (b) G8 (20% CLP @ 0° and 30% CLP @ 90°); (c) G9 (20% CLP @ 0° and 30% CLP @ 18°).

The main idea consists of extracting the amplitude and frequency of tooth in-plane bending vibration by numerical and experimental modal analysis. As well as a healthy gear (with no cracks), eight different gears were considered, with various crack scenarios in terms of number, depth, and location.

In the first part of this paper, a SolidWorks-based numerical investigation was made for all the gears previously mentioned. These simulation studies aimed to find the natural frequency of tooth bending with cracks and compare it to the healthy case. The simulation results clearly showed that the natural frequency of a cracked tooth's bending motion decreases if the CLP% increases. Such behavior is induced by a reduction in the stiffness of the tooth when a crack propagates deeper inside the tooth thickness. FEA was also used to calculate the deformation of the tooth. This deformation increases when the CLP% increases. Moreover, the simulation results showed a slight increase in the natural frequency of a cracked tooth if the crack is initiated through the rim.

The second part of the paper was devoted to an experimental investigation, which was needed to validate the numerical results found previously. The simulation results predetermined the fundamental parameters required for the experiments, such as the sampling frequency and the frequency range of interest. A test rig was designed, built, instrumented, and used to collect vibration responses resulting from hammer impact excitation. A set of FRF curves for healthy and damaged gears were obtained and superimposed on the same graphical representations. The experimental and numerical results agreed well in terms of both amplitudes and frequencies.

Finally, the representation of the tooth deformation and frequency in polar plots permitted straightforward and efficient qualitative identification of the location and extent of the cracked teeth.

Conflicts of interest

The authors declare that there is no conflict of interest.

Author Contributions

All authors contributed to this work and have read and agreed to the final published version of the manuscript.

Funding acknowledgement

This research did not receive any specific grant from any funding agency in the public, commercial, or not-for-profit sectors.

References

[1] J. J. Saucedo-Dorantes, M. Delgado-Prieto, R. A. Osornio-Rios, R. de J. Romero-Troncoso, "Diagnosis methodology for identifying gearbox wear based on statistical time feature reduction", *Proc. Inst. Mech. Eng., Part C: J. Mech. Eng. Sci.* **232** (2018), no. 15, p. 2711-2722.

[2] T. R. Praveenkumar, B. Sabhrish, M. Saimurugan, K. I. Ramachandran, "Pattern recognition based on-line vibration monitoring system for fault diagnosis of automobile gearbox", *Measurement* **114** (2018), p. 233-242.

[3] A. Fernandez del Rincon, F. Viadero, M. Iglesias, P. García, A. de Juan, R. Sancibrian, "A model for the study of meshing stiffness in spur gear transmissions", *Mech. Mach. Theory* **61** (2013), p. 30-58.

[4] R. Errichello, "Gear bending fatigue failure and bending life analysis", in *Encyclopedia of Tribology* (Q. J. Wang, Y. W. Chung, eds.), Springer, Boston, MA, 2013.

[5] S. Zouari, M. Maatar, T. Fakhfakh, M. Haddar, "Following spur gear crack propagation in the tooth foot by finite element method", *J. Fail. Anal. Prev.* **10** (2010), p. 531-539.

[6] X. Song, H. Ian, "Dynamic modeling of flexibly supported gears using iterative convergence of tooth mesh stiffness", *Mech. Syst. Signal Process.* **80** (2016), p. 460-481.

[7] S. Pehan, J. Kramberger, J. Flašker, B. Zafošnik, "Investigation of crack propagation scatter in a gear tooth's root", *Eng. Fract. Mech.* **75** (2006), no. 5, p. 1266-1283.

[8] C. Zaigang, S. Yimin, "Mesh stiffness calculation of a spur gear pair with tooth profile modification and tooth root crack", *Mech. Mach. Theory* **62** (2013), p. 63-74.

[9] Allianz Versicherungs-Aktiengesellschaft, *Handbook of Loss Prevention*, Springer, Berlin, 1978.

[10] S. Renping, D. Feifei, W. Wei, J. Purong, "Influence of cracks on dynamic characteristics and stress intensity factor of gears", *Eng. Fail. Anal.* **32** (2013), p. 63-80.

[11] Y. Pandya, A. Parey, "Failure path based modified gear mesh stiffness for spur gear pair with tooth root crack", *Eng. Fail. Anal.* **27** (2013), p. 286-296.

[12] A. Fernandez del Rincon, F. Viadero, M. Iglesias *et al.*, "A model for the study of meshing stiffness in spur gear transmissions", *Mech. Mach. Theory* **61** (2013), p. 30-58.

[13] A. De Luca, D. Perfetto, G. Petrone, A. De Fenza, F. Caputo, "Guided-waves in a low velocity impacted composite winglet", *Key Eng. Mater.* **774** (2018), p. 343-348.

[14] E. D. Lorenzo, G. Petrone, S. Manzato, B. Peeters, W. Desmet, F. Marulo, "Damage detection in wind turbine blades by using operational modal analysis", *Struct. Health Monit.* **15** (2016), no. 3, p. 289-301.
[15] X. Liang, H. Zhang, M. J. Zuo, Y. Qin, "Three new models for evaluation of standard involute spur gear mesh stiffness", *Mech. Syst. Signal Process.* **101** (2018), p. 424-434.
[16] L. Shuting, "Finite element analyses for contact strength and bending strength of a pair of spur gears with machining errors, assembly errors and tooth modifications", *Mech. Mach. Theory* **42** (2007), no. 1, p. 88-114.
[17] L. Shuting, "Effects of machining errors, assembly errors and tooth modifications on loading capacity, load-sharing ratio and transmission error of a pair of spur gears", *Mech. Mach. Theory* **42** (2007), no. 6, p. 698-726.
[18] H. Ma, J. Yang, R. Song, S. Zhang, B. Wen, "Effects of tip relief on vibration responses of a geared rotor system", *Proc. Inst. Mech. Eng., Part C: J. Mech. Eng. Sci.* **228** (2014), no. 7, p. 1132-1154.
[19] Z. Wang, H. Cao, Y. Zi, W. He, Z. He, "An improved TVMS algorithm and dynamic modeling of gear-rotor system with tooth root crack", *Eng. Fail. Anal.* **42** (2014), p. 157-177.
[20] L. Xihui, J. Z. Ming, P. Mayank, "Analytical evaluating the influence of crack on the mesh stiffness of a planetary gear set", *Mech. Mach. Theory* **76** (2014), p. 20-38.
[21] F. Chaari, W. Baccar, M. S. Abbes, M. Haddar, "Effect of spalling or tooth breakage on gear mesh stiffness and dynamic response of a one-stage spur gear transmission", *Eur. J. Mech. A/Solids* **27** (2008), no. 4, p. 691-705.
[22] F. Chaari, T. Fakhfakh, M. Haddar, "Analytical modeling of spur gear tooth crack and influence on gear mesh stiffness", *Eur. J. Mech. A/Solids* **28** (2009), no. 3, p. 461-468.
[23] D. C. H. Yang, J. Y. Lin, "Hertzian damping, tooth friction and bending elasticity in gear impact dynamics", *J. Mech. Des.* **109** (1987), no. 2, p. 189-196.
[24] S. Wu, M. J. Zuo, A. Parey, "Simulation of spur gear dynamics and estimation of fault growth", *J. Sound Vib.* **317** (2008), no. 3–5, p. 608-624.
[25] O. D. Mohammed, M. Rantatalo, J. A. Aidanpää, U. Kumar, "Vibration signal analysis for gear fault diagnosis with various crack progression scenarios", *Mech. Syst. Signal Process.* **41** (2013), no. 1–2, p. 176-195.
[26] O. D. Mohammed, M. Rantatalo, "Gear fault models and dynamics-based modelling for gear fault detection—A review", *Eng. Fail. Anal.* **117** (2020), article no. 104798.
[27] C. Zaigang, S. Yimin, "Dynamic simulation of spur gear with tooth root crack propagating along tooth width and crack depth", *Eng. Fail. Anal.* **18** (2011), no. 8, p. 2149-2164.
[28] O. D. Mohammed, M. Rantatalo, J. O. Aidanpää, "Improving mesh stiffness calculation of cracked gears for the purpose of vibration-based fault analysis", *Eng. Fail. Anal.* **34** (2013), p. 235-251.
[29] O. D. Mohammed, M. Rantatalo, "Gear tooth crack detection using dynamic response analysis", *Insight, Non-Destr. Test. Cond. Monit.* **55** (2013), no. 8, p. 417-421.
[30] O. D. Mohammed, M. Rantatalo, "Dynamic response and time-frequency analysis for gear tooth crack detection", *Mech. Syst. Signal Process.* **66–67** (2016), p. 612-624.